

# Genome-wide analysis of ETS-family DNA-binding *in vitro* and *in vivo*

This is an open-access article distributed under the terms of the Creative Commons Attribution Noncommercial Share Alike 3.0 Unported License, which allows readers to alter, transform, or build upon the article and then distribute the resulting work under the same or similar license to this one. The work must be attributed back to the original author and commercial use is not permitted without specific permission.

Gong-Hong Wei<sup>1</sup>, Gwenaél Badis<sup>2</sup>,  
Michael F Berger<sup>3,4,5,6</sup>, Teemu Kivioja<sup>1,7</sup>,  
Kimmo Palin<sup>7</sup>, Martin Enge<sup>8</sup>,  
Martin Bonke<sup>1</sup>, Arttu Jolma<sup>1</sup>,  
Markku Varjosalo<sup>1</sup>, Andrew R Gehrke<sup>3,4,5,6</sup>,  
Jian Yan<sup>1</sup>, Shaheynoor Talukder<sup>2</sup>,  
Mikko Turunen<sup>1</sup>, Mikko Taipale<sup>1</sup>,  
Hendrik G Stunnenberg<sup>9</sup>, Esko Ukkonen<sup>7</sup>,  
Timothy R Hughes<sup>2</sup>, Martha L Bulyk<sup>3,4,5,6</sup>  
and Jussi Taipale<sup>1,8,\*</sup>

<sup>1</sup>Public Health Genomics Unit, National Institute for Health and Welfare (THL) and Genome-Scale Biology Program, Institute of Biomedicine and High Throughput Center, University of Helsinki, Biomedicum, Helsinki, Finland, <sup>2</sup>Department of Molecular Genetics and Banting and Best Department of Medical Research, University of Toronto, Toronto, Ontario, Canada, <sup>3</sup>Division of Genetics, Department of Medicine, Brigham and Women's Hospital and Harvard Medical School, Boston, MA, USA, <sup>4</sup>Department of Pathology, Brigham and Women's Hospital and Harvard Medical School, Boston, MA, USA, <sup>5</sup>Committee on Higher Degrees in Biophysics, Harvard University, Cambridge, MA, USA, <sup>6</sup>Harvard-MIT Division of Health Sciences and Technology (HST), Harvard Medical School, Boston, MA, USA, <sup>7</sup>Department of Computer Science, University of Helsinki, Helsinki, Finland, <sup>8</sup>Department of Biosciences and Medical Nutrition, Karolinska Institutet, Sweden and <sup>9</sup>Department of Molecular Biology, Radboud University Nijmegen, Nijmegen, The Netherlands

Members of the large ETS family of transcription factors (TFs) have highly similar DNA-binding domains (DBDs)—yet they have diverse functions and activities in physiology and oncogenesis. Some differences in DNA-binding preferences within this family have been described, but they have not been analysed systematically, and their contributions to targeting remain largely uncharacterized. We report here the DNA-binding profiles for all human and mouse ETS factors, which we generated using two different methods: a high-throughput microwell-based TF DNA-binding specificity assay, and protein-binding microarrays (PBMs). Both approaches reveal that the ETS-binding profiles cluster into four distinct classes, and that all ETS factors linked to cancer, ERG, ETV1, ETV4 and FLI1, fall into just one of these classes. We identify amino-acid residues that are critical for the differences in specificity between all the classes, and confirm the specificities *in vivo* using chromatin immunoprecipitation followed by sequencing (ChIP-seq) for a member of each class. The results indicate that even relatively small differences

in *in vitro* binding specificity of a TF contribute to site selectivity *in vivo*.

The EMBO Journal advance online publication, 1 June 2010;  
doi:10.1038/emboj.2010.106

Subject Categories: chromatin & transcription; genomic & computational biology

Keywords: cancer; ChIP-seq; DNA-binding specificity; ETS family of transcription factors; transcription factor-DNA binding assay

## Introduction

We currently know very little about the molecular mechanisms that control tissue-specific gene expression, and about the variations in gene expression that underlie many pathological states, including cancer. This is in part due to the lack of information about the 'second genetic code'—the binding specificities of transcription factors (TFs). Deciphering this regulatory code will allow us to explain observations (i.e. ChIP, expression profiling) based on biochemical principles. The ultimate aim is to read the genetic code of gene expression, that is, understand the expression of genes based on DNA sequence.

To begin to address these questions, we have in this work concentrated on the study of the large ETS family of TFs, whose members have diverse functions and activities in physiology and oncogenesis (Bartel *et al*, 2000; Sharrocks, 2001; Kumar-Sinha *et al*, 2008). The first ETS factor identified was ETS1, which was discovered as a homolog of the avian leukaemia virus E26 oncogene in 1983 (Leprince *et al*, 1983; Nunn *et al*, 1983). Subsequent analyses have identified a total of 27 and 26 ETS-family members in human and mouse genomes, respectively (Bult *et al*, 2008).

ETS factors have both developmental functions (Schober *et al*, 2005), and functions in differentiated tissues and cells (Bartel *et al*, 2000). They are critical for vasculogenesis/angiogenesis, hematopoiesis and neuronal development (Bartel *et al*, 2000; Vrieseling and Arber, 2006). Cellular responses to activated ETS factors include cell proliferation, differentiation and migration (Sharrocks, 2001; Schober *et al*, 2005), depending on the type and state of the responding cell.

Many ETS proteins, including ETV4 in mammals and Yan in *Drosophila* are transcriptional targets of signalling pathways (Schober *et al*, 2005; Vrieseling and Arber, 2006). Activity of ETS proteins can also be modulated directly by phosphorylation; members of the ETS and ELK subgroups of ETS factors mediate transcriptional responses to Ras/MAPK signalling pathways in species ranging from *Caenorhabditis elegans* to humans (Brunner *et al*, 1994; O'Neill *et al*, 1994;

\*Corresponding author. Department of Biosciences and Medical Nutrition, Karolinska Institutet, Sweden. Tel.: +46 858 583 833; E-mail: jussi.taipale@ki.se

Beitel *et al*, 1995; Sharrocks, 2001). The mechanism of activation of the ELK factors in response to activation of Ras also appears to be conserved between species (Wasylyk *et al*, 1997).

Translocations altering the activity of several members of the ETS family are associated with multiple types of human cancer. In translocations observed in some cancer types, the ETS DNA-binding domain (DBD) is lost, and the ETS partner contributes a regulatory domain to another class of DBD (e.g. ETV6-RUNX1; Golub *et al*, 1995; Mavrothalassitis and Ghysdael, 2000). More commonly, the cancer-associated translocations result in fusion of a strong transcriptional activator domain to the ETS DBD (e.g. EWS fused to FLI1 or ERG in Ewing's sarcoma; Delattre *et al*, 1992; Sorensen *et al*, 1994) and/or overexpression of an ETS-family member due to introduction of a strong *cis*-regulatory element upstream of it (Tomlins *et al*, 2005, 2007). In fact, the most common known cancer-associated translocation is the TMPRSS2-ERG fusion, which introduces a strong androgen receptor (AR)-dependent regulatory element upstream of the ERG gene (Tomlins *et al*, 2005). Together with other translocations involving ETV1 and ETV4, over 50% of all prostate cancer cases display hyperactivity of ETS proteins (Kumar-Sinha *et al*, 2008).

All ETS factors share a conserved winged helix-turn-helix DBD of ~85 amino acids, and all analysed members of this family bind to a consensus DNA sequence containing a core 5'-GGA(A/T)-3' motif (Karim *et al*, 1990; Nye *et al*, 1992). On the basis of phylogenetic analysis of the DBDs, the ETS family has been subdivided into 12 different subgroups (Laudet *et al*, 1999; Hollenhorst *et al*, 2007). Thus, although all ETS DBDs are relatively highly conserved, different ETS proteins might exhibit a preference for different flanking sequences to differentially bind to specific DNA sites, and thus regulate distinct biological processes. However, there exists no systematic and uniform analysis of ETS-binding specificities, and whether differences in binding specificity (if any) relate to targeting *in vivo*. An earlier analysis showed that there were differences between published motifs for different ETS-family members, but these differences did not reflect amino-acid features, and might be due to differences in the experimental methods used in different studies (Kielbasa *et al*, 2005).

In this work, we describe the first comprehensive genome-wide analysis of binding specificities of the ETS TF family. We find that the ETS-family DNA-binding specificities fall into four distinct classes, and confirm this finding by identifying the key DNA-contact amino acids that contribute to class specificity. We further perform ChIP-seq analyses for representative ETS factors to map the ETS-binding sites *in vivo* in Ewing's sarcoma, leukaemia and prostate cancer cells. These analyses provide a systematic genome-wide map of ETS DNA-binding specificities *in vitro* and *in vivo*. Remarkably, the genome-wide data reveal that even small differences in ETS DNA-binding preferences can contribute to *in vivo* targeting specificities.

## Results

### Systematic determination of ETS-binding specificities

To determine the binding specificities of the ETS factors, we first cloned all human and mouse ETS DBDs and human ETS full-length cDNAs (Figure 1; Supplementary Table S1). Two

parallel methods were used to independently determine relative DNA sequence-specific binding affinities: high-throughput microwell-based TF DNA-binding specificity assay (Hallikas and Taipale, 2006; Hallikas *et al*, 2006) and protein-binding microarrays (PBMs; Berger *et al*, 2006). As these two strategies are based on different principles, they act to complement and cross-validate each other.

In the microwell-based assay, human and mouse ETS DBDs were expressed as fusion proteins to a *Renilla* luciferase enzyme. The TF-*Renilla* luciferase fusion proteins were incubated with biotinylated double-stranded oligonucleotide containing a sequence with high affinity to all known ETS factors in the presence of an excess of mismatched competitor oligos. The binding data were then analysed to produce a position weight matrix (PWM) of the TF-binding site.

Independent analysis of the mouse ETS family was carried out using PBMs, which allow determination of TF-binding specificities through sequence-specific binding of individual TFs directly to double-stranded DNA microarrays containing all possible 10-mer binding sites (Berger *et al*, 2006).

Both methods generated similar binding profiles (Figure 1; Supplementary Table S2), with all of the ETS factors binding to the previously described core GGA(A/T) motif. Of the 27 factors we studied, 13 had been previously analysed using different methods to yield a partial binding specificity. Our results were similar, but not identical, to these earlier studies, as described in the following sections.

### Analysis of the divergence of ETS TF-binding profiles

We next analysed the differences in the obtained profiles to determine which ETS factors have similar binding specificities. For this purpose, we developed a computational method that allows determination of similarity between TF motifs using the minimum Kullback–Leibler divergence between all translations and reverse complementations of the multinomial distributions defined by the motifs. This analysis revealed that all ETS profiles were relatively similar to each other, and clearly divergent from publicly available non-ETS TF-binding profiles (Figure 2). The ETS-binding profiles fell into four distinct classes (Figure 2), containing 15, 8, 3 and 1 member(s), respectively. These classes were robustly identified using results either only from the microwell-based method (Figure 2), from only the PBM method (Figure 3A and B) or from the combination of the two (Supplementary Figure S1A). The classes were named according to their respective sizes, with class I being the largest group, containing the cancer-associated ETS factors ERG, ETV1, ETV4 and FLI1. Consistent with earlier results (Kielbasa *et al*, 2005), clustering analysis of ETS factors available from current databases and literature did not yield a clear classification of sites (Figure 3C; Supplementary Figure S3). However, the classes we obtained do show a clear relationship to groupings based on amino-acid features (see below and Discussion).

The main differences between our motifs are concentrated on the core +4 position and 5' flanking base pairs. Although the consensus sequences of the ETS factors are relatively similar, many somewhat weaker sites are much more class specific or exclude one or more classes of ETS DBDs (Supplementary Figure S2). Only the difference between other ETS-family members analysed and the lone class IV factor SPDEF has been identified earlier (Oettgen *et al*, 2000).

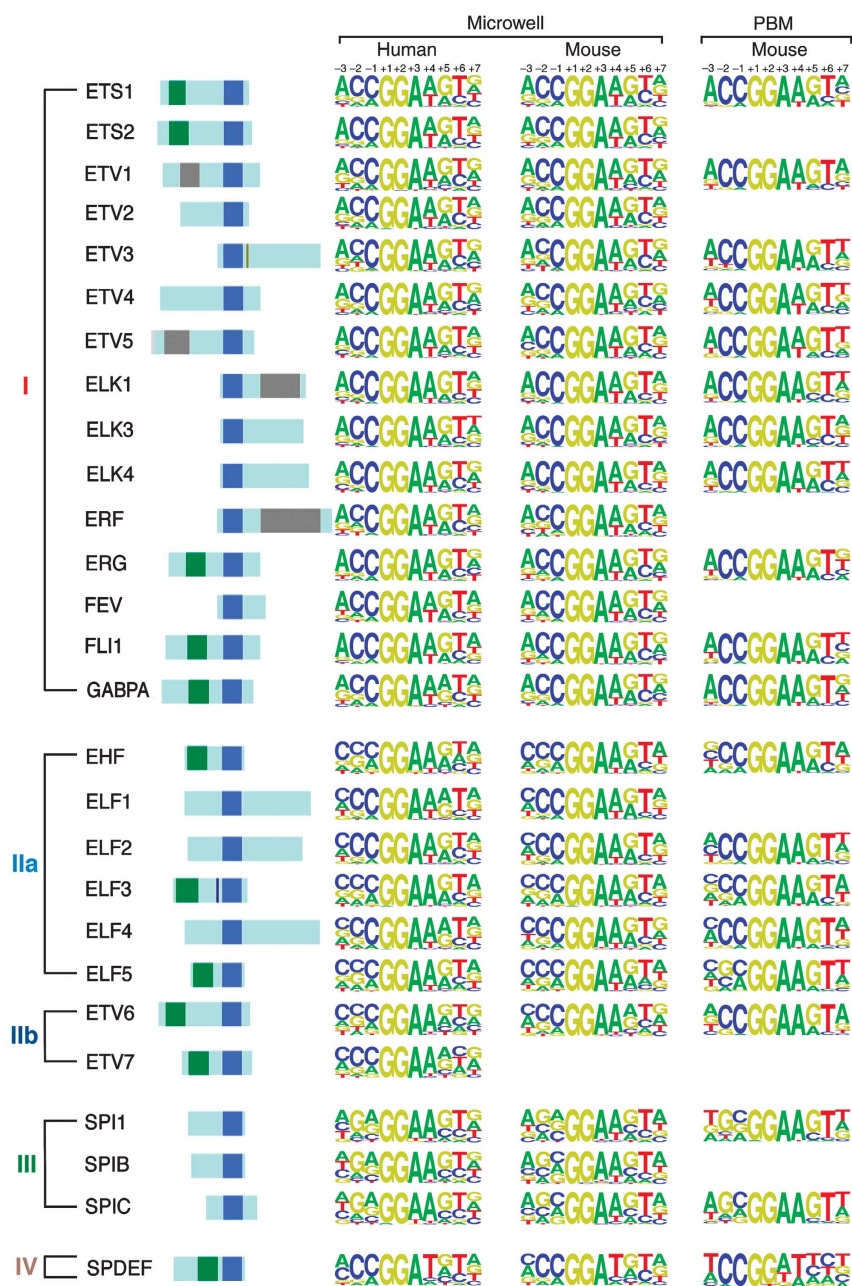


**Figure 1** Structural organizations and binding specificities of mammalian ETS transcription factors. (Left) Schematic representation of the domain structures of the respective full-length proteins. ETS domain is in blue, pointed domain is in green, Proline-rich domain is in grey, and the Nuc\_orp\_HMR\_rcpt and A/T hook domains are in dark yellow and black, respectively. HUGO gene names are from ENSEMBL and protein domains are from Pfam. The second and third columns, respectively, show human and mouse ETS-binding profiles determined using microwell-based transcription factor-DNA-binding assays. The right column shows mouse ETS-binding profiles determined using protein-binding microarrays. The logos are drawn using enoLOGOS (Workman *et al*, 2005), and the height of a letter at a particular position is directly proportional to the effect of that nucleotide on the binding affinity. Coordinates for the bases are also indicated above each column (see also Supplementary Figures S1 and S9; Supplementary Tables S1, S2 and S6; Supplementary data file S1).

In general, the class definitions derived using hierarchical clustering seemed to be largely sufficient to explain the differences between the ETS-family members. However, ETV6 and ETV7 appeared to have subtly different binding specificity at +4 compared with the other members of class II (Figure 1), and in this way resembled more the class III factors. We therefore propose subclassification of class II into class IIa containing the ELF-family factors, and class IIb comprising ETV6 and ETV7.

### Molecular basis of ETS-class specificity

To analyse the molecular basis of the differences in ETS-binding specificities, we investigated the amino acid-DNA contacts in published crystal structures of ETS1, GABPA, ELK1, ELF3, SPI1 and SPDEF-DNA complexes (Kodandapani *et al*, 1996; Batchelor *et al*, 1998; Mo *et al*, 1998, 2000; Garvie *et al*, 2001; Verger and Duterrque-Coquillaud, 2002; Pufall *et al*, 2005; Wang *et al*, 2005; Lamber *et al*, 2008; Agarkar *et al*, 2010). The invariant GGA



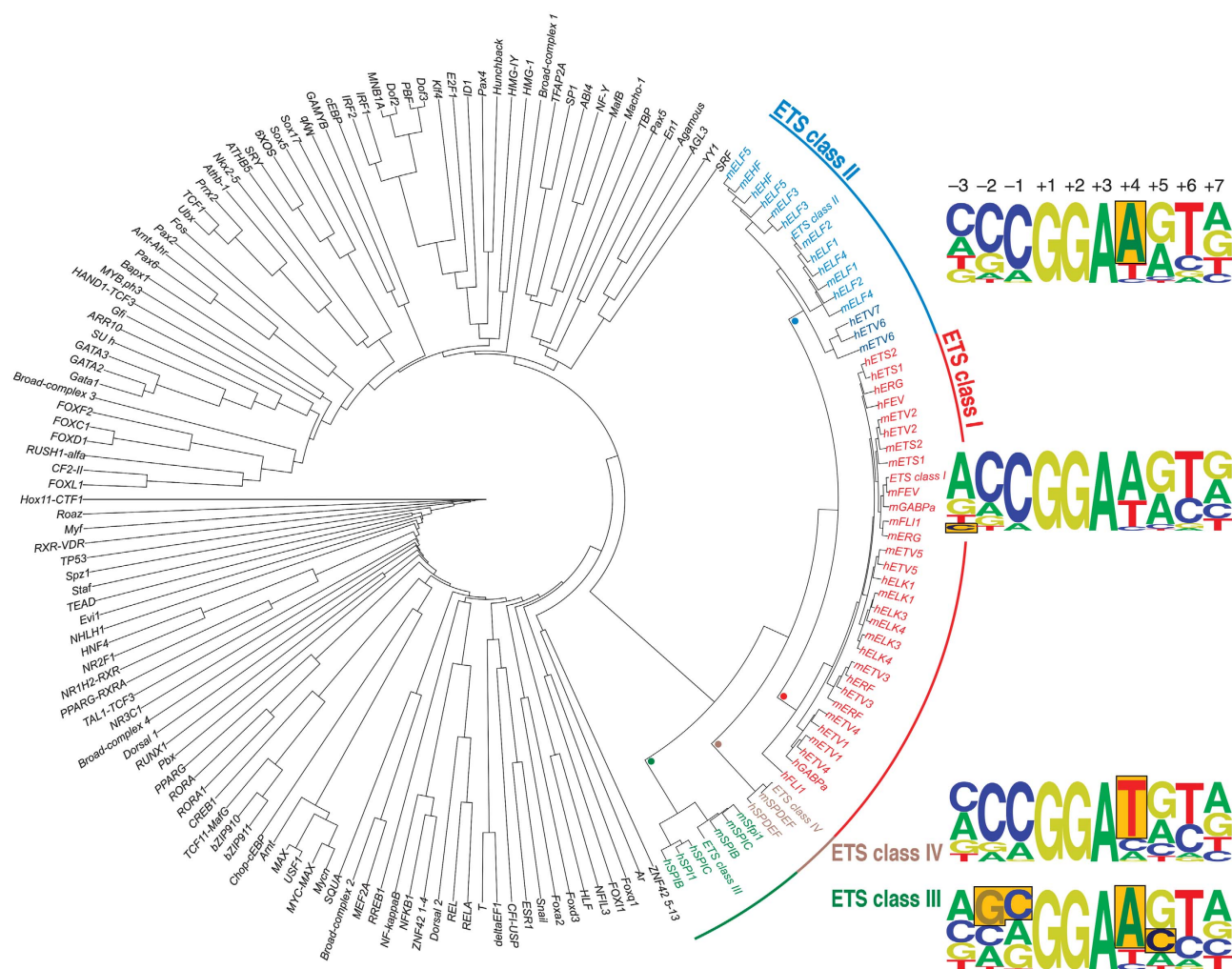


**Figure 2** ETS-binding specificity. Clustering analysis of binding profiles of human (h) and mouse (m) ETS transcription factors (microwell method) and publicly available non-ETS-family transcription factor matrices from Jaspar2 (Bryne *et al*, 2008; <http://jaspar.genereg.net>). The four different classes of ETS factors are indicated by colour: class I, red; class II, blue; class III, green; class IV, brown. Coloured dots indicate the main branches defining the classes. ETS matrices indicated as 'class' are the representative matrices for the different ETS classes identified using affinity propagation clustering (see Materials and methods for details). Representative logos, drawn using enoLOGOS (Workman *et al*, 2005), are also shown. Bases displaying the most prominent changes are boxed (see also Supplementary Figures S2 and S6; Supplementary data file S1).

core bases of the ETS-family profiles are consistent with the absolute conservation of two key DNA-contacting arginines in Helix3 (Figure 4A, black). Most of the differences in DNA-binding specificity at particular bases, in turn, correlate with corresponding changes in residues contacting DNA at or near these bases (Figure 4B). The preference of the lone class IV factor, SPDEF for T at +4 correlates with the presence of serine and glutamine at DNA-contact residues 9 and 11, respectively. Recent crystal structure analysis of SPDEF-DNA complex suggested that combination of these residues is responsible for the preference of T at +4 (Wang *et al*, 2005). We confirmed the importance of these two residues by mutagenesis followed by microwell-based DNA-binding specificity assay (Figure 4C).

Class I factors are characterized by low affinity to C in the −3 position. This change correlates with a substitution of a leucine that contacts DNA backbone at −2 and −3 with a phenylalanine or tyrosine (Figure 4B, red). Mutation of the leucine residue to either tyrosine or phenylalanine in

the context of the class II factor ELF4-DBD resulted in a clear shift of specificity towards class I at −3 position, confirming the importance of this amino acid for the differences in specificity between class I and the other classes (Figure 4D).

Whereas Class IIa factors did not have major features that differentiated them from all other classes, class IIb factors displayed strong preference for A at +4. This change correlated with a substitution of a key tyrosine by a histidine. Mutation of this residue in ELF4-DBD increased binding to sequences containing A at +4, confirming the importance of this residue in class IIb specificity (Figure 4D).

Class III factors were characterized by preference of G and C at −2 and −1, respectively, strong preference for A at +4, and relatively strong binding of sites with a C at +5. Many amino-acid residues within the DBD are specific for class III (Figure 4B). As the tyrosine that affects specificity at +4 is replaced in class III by an asparagine, we first investigated the function of this amino-acid change. Mutating the tyrosine to

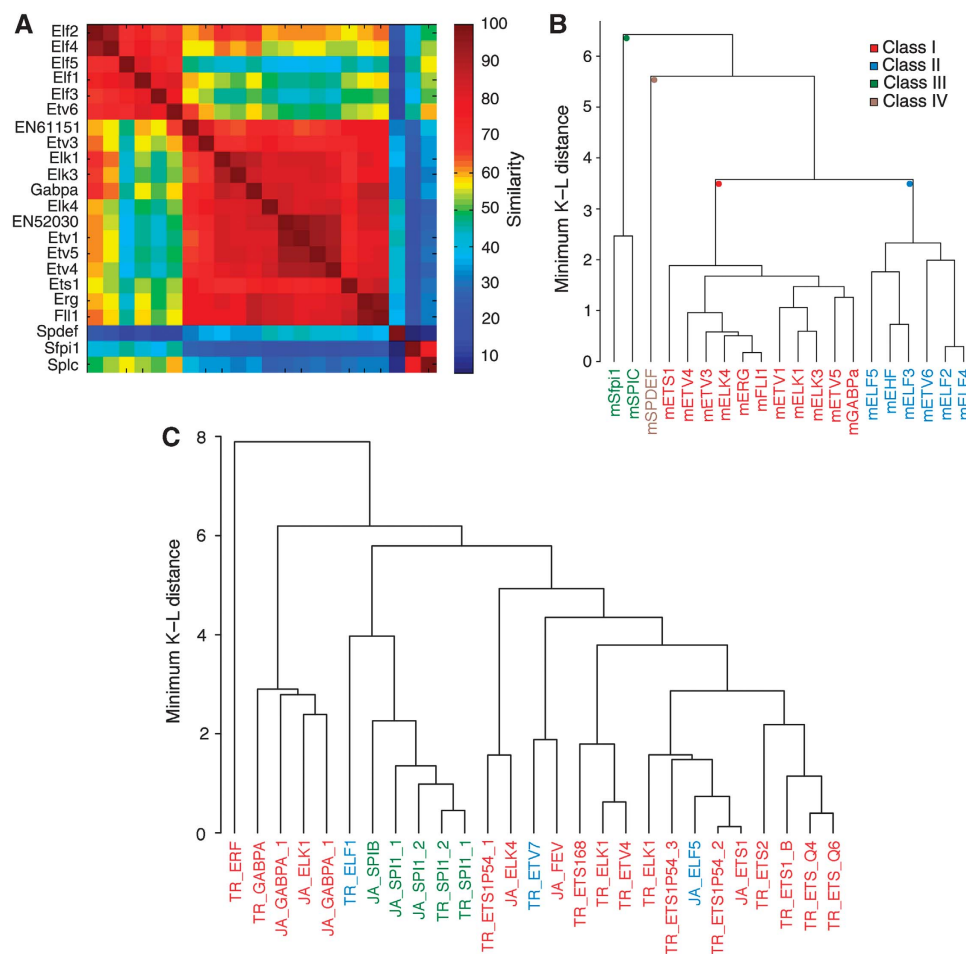


**Figure 3** Identification of four ETS classes is independent of clustering and binding model derivation methods used. **(A)** Heat-map correlation analysis of the protein-binding microarray-derived ETS-binding models. The same four ETS classes are detected when protein-binding microarray results are clustered using the top 100 TF-binding sites for each ETS-family member (analysis as in Berger *et al*, 2008). In all, 20 known and 2 predicted mouse ETS-family members are included in the analysis. **(B)** Kullback–Leibler divergence-based clustering analysis of mouse ETS-binding profiles derived from protein-binding microarrays. Note that this analysis also reveals the same four different classes of ETS factors, which are indicated in the same colours as in Figures 1 and 2. Coloured dots indicate the main branches defining the classes. **(C)** Clustering of existing ETS family binding profiles from JASPAR2 (JA), TRANSFAC (TR) professional and literature (Nye *et al*, 1992; Treisman *et al*, 1992; Woods *et al*, 1992; Dalton and Treisman, 1992; Virbasius *et al*, 1993; Ray-Gallet *et al*, 1995; Shore and Sharrocks, 1995; Matys *et al*, 2006; Choi and Sinha, 2006; Bryne *et al*, 2008). Note that the four separate ETS classes are not identified using the earlier data (see also Supplementary Figures S3 and S6).

an asparagine in ELF4-DBD led to a clear change of specificity towards that of class III both at +4 and +5 (Figure 4D).

Preference for G at −2 in class III could, in turn, be due to substitution of a tyrosine—which contacts the DNA backbone between bases −1 and −2—with a glycine or an alanine (Figure 4B). However, mutation of this residue in ELF4-DBD to either glycine or alanine had no impact on specificity. In contrast, mutation of a class III-specific glutamate that contacts water molecule between positions −1 and 1 (Kodandapani *et al*, 1996) to a glutamine residue led to a clear change of specificity of ELF4 towards class III at positions −1 and −2 (Figure 4D).

Taken together, these results indicate that the ETS DNA-binding specificities fall into four clearly distinct classes (Figures 2, 3A and B), and that the molecular mechanisms of the differences in four kinds of ETS-binding motifs are due to amino-acid divergences at defined DNA-contacting residues (marked 5, 9, 11 and 14 in Figure 4A). The observed changes in binding specificity are also consistent with crystal

structures for the ETS-family members (see Figure 5; Kodandapani *et al*, 1996; Batchelor *et al*, 1998; Mo *et al*, 1998; Mo *et al*, 2000; Garvie *et al*, 2001; Pufall *et al*, 2005; Wang *et al*, 2005; Lamber *et al*, 2008; Agarkar *et al*, 2010).

### ChIP-seq of ETS-binding sites *in vivo*

To further validate the binding profiles, and to examine binding of ETS factors to DNA *in vivo*, we used ChIP-seq to determine occupied sites for each class of ETS factors in cell lines. Antibodies to endogenous proteins were used in all experiments. Class I and class IV factors ERG and SPDEF were analysed in the androgen-dependent prostate cancer cell line VCaP, and the class II and class III factors ELF1 and SPI1 were analysed in leukaemia cell lines Jurkat and HL60, respectively. In addition, we included in the analysis two oncogenic ETS-fusion proteins, EWS/ERG and EWS/FLI1, which were analysed in the Ewing's sarcoma cell lines CADO-ES1 and SK-N-MC, respectively. We also performed ChIP-seq using two additional antibodies in VCaP cells,

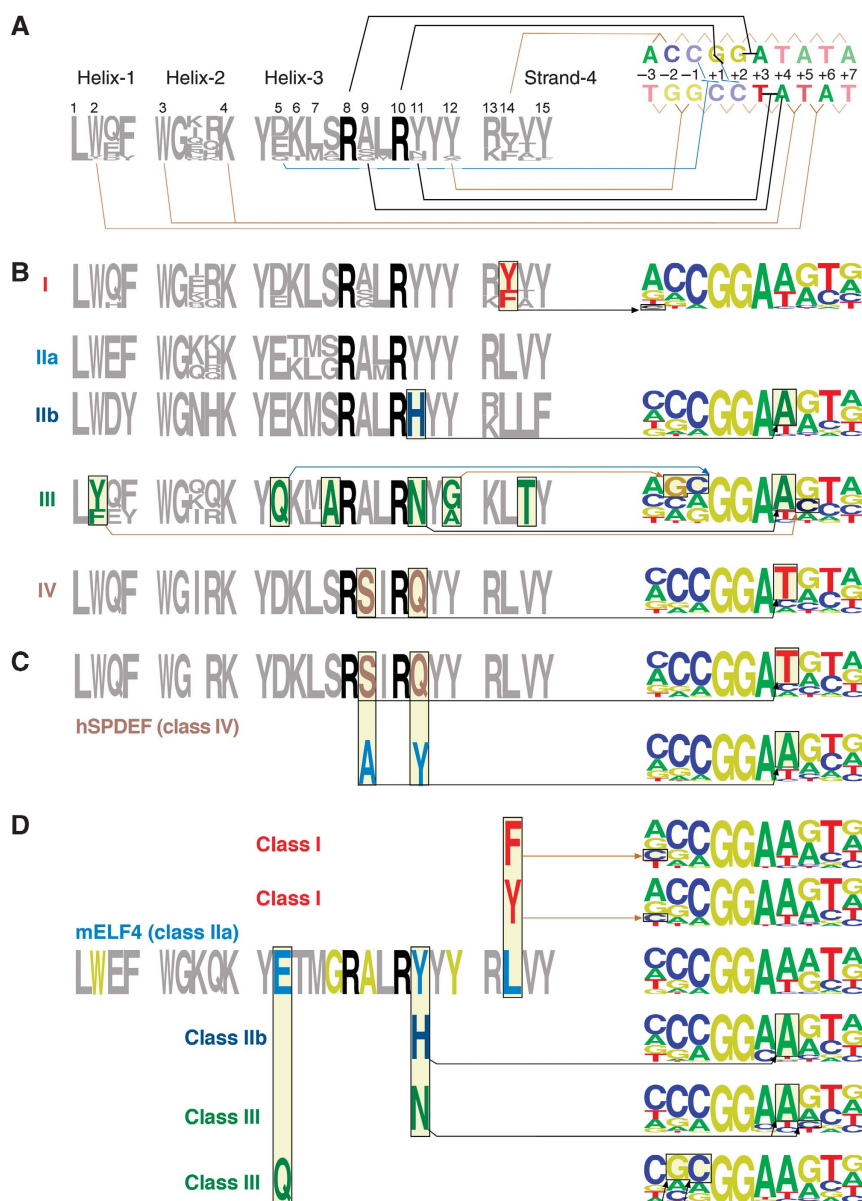


**Figure 4** Molecular basis of ETS-class specificity. (A) ETS-domain secondary structure indicating key amino acids contacting nucleotide bases (black lines), DNA-backbone (brown lines) and water (blue line) based on the published crystal structures of ETS-domain DNA complexes (Kodandapani *et al*, 1996; Batchelor *et al*, 1998; Mo *et al*, 1998, 2000; Garvie *et al*, 2001; Pufall *et al*, 2005; Wang *et al*, 2005; Lamber *et al*, 2008; Agarkar *et al*, 2010). Amino-acid residues contacting DNA are numbered from 1 to 15. Two invariant arginines that bind to the core GGA sequence are in black typeface. Bases contributing to DNA-binding specificity are numbered from -3 to +7. (B) (Left) Sequence logos showing amino-acid conservation in DNA-contacting regions of the different ETS classes. Amino acids that are specific for a given class are indicated by colours, and the two invariant arginines are in black. (Right) Representative PWMs for the ETS classes. Bases that distinguish each class from the others are boxed, and residues that contact bases, water or DNA backbone are indicated in black, blue or yellow lines, respectively. (C) Identification of amino-acid residues that are required for class IV DNA-binding specificity. Mutating key DNA-contact residues in ETS class IV factor SPDEF (top) to the corresponding residues in ETS class IIa (bottom left) results in a change in DNA-binding specificity of SPDEF towards class IIa (bottom right; data from microwell assay). (D) Identification of amino-acid residues that can confer class I, IIb or III DNA-binding specificity to a class IIa ETS DNA-binding domain from mouse ELF4 were mutated to the corresponding residues in the other ETS classes. The resulting DNA-binding profile from microwell assay is shown on the right. Bases displaying the most prominent changes are boxed. Note that one or two amino-acid mutations can move the specificity of ELF4 towards the other ETS classes. Residues whose mutation to the corresponding residues in class III had no effect on specificity are indicated in yellow.

histone H3 lysine 4 monomethylation to identify potential enhancers, and the non-ETS TF, AR, which served as a positive control. IgG was used as a negative control in all cell lines (see Materials and methods for details). Analysis of the results revealed between 2142 (ERG) and 98 290 (H3K4 monomethylation) significantly enriched regions ( $P < 0.005$ ), which we refer to as 'peaks' hereafter (Supplementary Table

S4; Supplementary data files S2–S9). Randomly selected ChIP-seq peaks were confirmed using ChIP-qPCR (see Materials and methods; Supplementary Table S5 for details).

For the ETS-fusion proteins EWS/FLI1 and EWS/ERG, the ChIP-seq peaks were located relatively evenly in the genome. The non-fusion ETS-family factors ERG, SPDEF and SPI1 demonstrated a relatively small enrichment near transcrip-



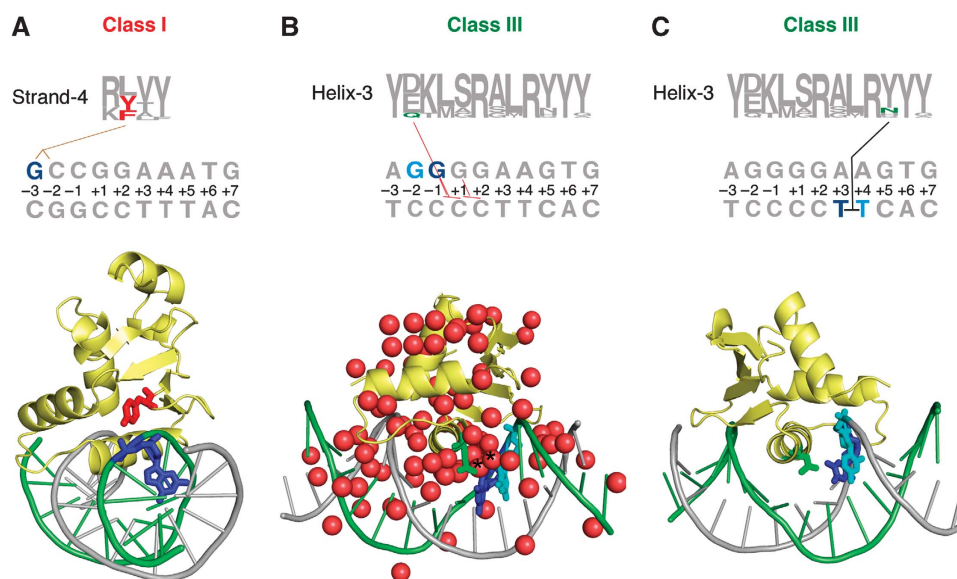


**Figure 5** Crystal structures displaying residues that are critical for ETS-class specificity. (A) Tyrosine 410 (red) in strand-4 of ETS1 (class I) contacting DNA backbone between positions  $-3$  and  $-2$  (base G at  $-3$  indicated in blue). This residue is responsible for exclusion of C at position  $-3$ . (B) Glutamine 228 in helix-3 of SPI1 (class III) contacting water molecules (red spheres indicated by asterisks) near DNA positions  $-1$  (blue) and  $-2$  (cyan). This residue is responsible for preference of G at  $-2$ , and weaker binding to C at  $-1$ . (C) Asparagine 236 in helix-3 of SPI1 (class III) contacting an adenine at  $+4$  position. This residue is responsible for stronger preference for A at  $+4$  and higher-affinity binding to sites containing a C at  $+5$ . Top parts of each panel display sequence logos for the classes and the DNA sequences used in the crystallization (Kodandapani *et al*, 1996; Garvie *et al*, 2001), with the class-specific amino-acid residues and bases indicated by colouring. Contacts between amino acids and DNA backbone, water or bases are indicated using brown, red or black lines, respectively. Images were generated using PolyView-3D (<http://polyview.cchmc.org/polyview3d.html>).

tion start sites, whereas ELF1 displayed a very strong preference for binding near TSSs (Figure 6A; Supplementary Table S4). Consistent with earlier results, we also observed an enrichment of peaks within potential enhancer elements identified by proximity to nucleosomes where Histone H3 lysine 4 is monomethylated (Supplementary Table S4; Heintzman *et al*, 2007; Hollenhorst *et al*, 2009).

To determine whether the ChIP-seq peaks were near genes regulated by the respective ETS factors, we used RNAi to downregulate FLI1 in SK-N-MC Ewing's sarcoma cells. Two different siRNAs were used to rule out off-target effects (Echeverri *et al*, 2006), and two biological replicates were used for each siRNA to decrease noise. The affected genes included novel and previously known targets of FLI1 (Tirode *et al*, 2007; Supplementary Table S3). FLI ChIP-seq peaks were strongly enriched near transcription start sites of the FLI1-target genes (Figure 6B). Although the FLI1 peaks in general were distributed relatively evenly in the genome, the enrichment of FLI1 peaks near target genes was strongest very close to the TSS, suggesting that many of the more distal peaks have little impact on transcription, whereas more proximal peaks are more likely to affect gene regulation.

#### Analysis of specificity of ETS-family members *in vivo*

Given the relatively similar DNA-binding specificities of all the ETS-family members, an important question is whether the specificity of binding comes from the observed relatively small differences in protein–DNA binding affinity, or whether direct protein–protein interactions, or more complex chromatin-mediated effects dominate.

To address this, we analysed the ChIP-seq peak sequences to determine the relative enrichment of sequences that bind with high affinity to the different ETS classes *in vitro*.

All ChIP-seq peak sequences were strongly enriched in matches to matrices representing specific ETS classes, and in each case, the most enriched class corresponded to the class of the factor analysed by ChIP-seq (Figure 6C).

To analyse the sequence characteristics of the peaks further, we selected sequences from the 150 most significant peaks that were narrower than 400 bp for each ChIP-seq experiment. Searching these sequences for overrepresented motifs using MEME (Bailey and Elkan, 1994) revealed a clear ETS-family signature in experiments analysing each ETS class. The bases characteristic for the different ETS classes were also confirmed by the MEME analysis (Figure 6D). However, consistent with earlier results for FLI1 (Gangwal *et al*, 2008), analysis of EWS/ERG and EWS/FLI1 peak sequences resulted in identification of a motif resembling GGAA microsatellite repeats (Supplementary Figure S8A). This result suggests that the EWS-fusion alters the binding site selectivity of the ETS proteins.

Although high-affinity *in vitro* sites were strongly enriched near the summits of the ChIP-seq peaks, only a small fraction of such sites in the whole genome were occupied in the cell lines tested. In ERG and SPDEF ChIP-seq peaks from VCaP, the fraction of high-affinity sites that were occupied was much higher within 500 bp of regions that were positive for histone H3 lysine 4 monomethylation, a known marker for nucleosomes that flank enhancer regions (Heintzman *et al*, 2007; Supplementary Table S4). These results suggest that accessibility of DNA is a major determinant of site occupancy.

#### Overlap between different classes of ETS factors

We next analysed the overlap between the sites occupied by the ETS factors (Figure 7A). As expected, analysis of the same

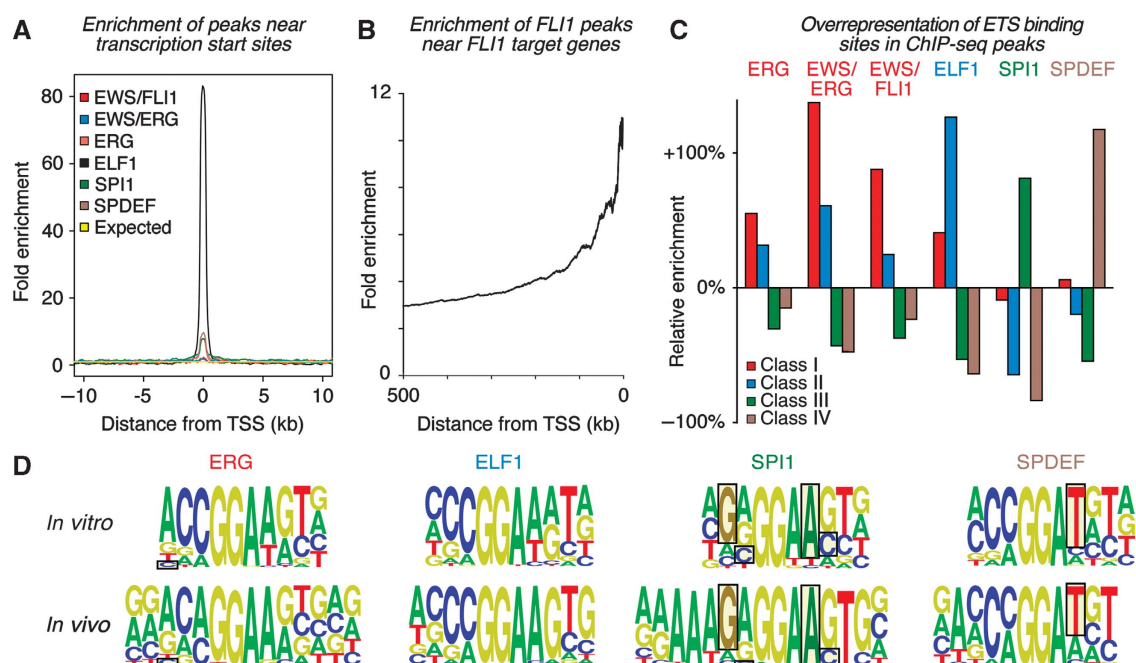


**Figure 6** ChIP-seq analysis of the different ETS classes. (A) Relative enrichment of ChIP-seq peaks with respect to transcription start sites. Note that ELF1 peaks are strongly enriched in promoters, whereas the other non-fusion ETS-family factors ERG, SPDEF and SPI1 display smaller promoter enrichment. The ETS factors fused to the EWS protein (EWS/FLI1 and EWS/ERG) display the smallest enrichment at promoters. (B) Enrichment of FLI1 ChIP-seq peaks near transcription start sites of genes that are downregulated in response to FLI1 siRNAs. (C) Analysis of specific enrichment of ETS class PWM matches in ChIP-seq peak sequences. Note that sequences immunoprecipitated using antibodies against a member of a given ETS DNA-binding class are enriched in matches to the PWM representing the same class. (D) MEME analysis of enrichment of sequence motifs in ChIP-seq peaks from experiments analysing members of all ETS classes (ERG, ELF1, SPI1 and SPDEF). Note that peaks in ChIP-seq experiments are enriched in motifs (*in vivo*, bottom) that are similar to those obtained using microwell assay (*in vitro*, top). Note also that the *in vivo* analysis confirms the differences in specificity of the ETS classes at the class-specific positions (boxes; see Figure 2) identified *in vitro*. The differences observed between the *in vitro* and *in vivo* profiles mainly affect the −1 and +5 positions of ERG and ELF1, respectively. These differences could be at least in part due to the presence of a high number of GGAA repeat containing ETS sites in the human genome, as −1 and +5 positions in sites derived from such repeats are enriched in A and G, respectively. These GGAA repeat-derived sequences can be functionally important (Gangwal *et al*, 2008). Colour code: class I, red; class II, blue; class III, green; class IV, brown (see also Supplementary Figures S8 and S10; Supplementary Tables S3–S6; Supplementary data files S2–S8).

factor in different cells (ERG in VCaP and CADO-ES1) or different factors in the same (ERG and SPDEF both in VCaP) or similar (FLI1 and ERG in Ewing's sarcoma; ELF and SPI1 in leukaemia) type of cell appeared to increase overlap of the peaks. Still, the majority of the peaks were specific in all experiments, with overlap ranging between 0.9% (EWS/FLI1 and SPDEF) and 25.8% (ERG and SPDEF). Strikingly, overlap between ERG peaks from VCaP and the control AR peaks was much higher than for any other pair of factors; 44.4% of all ERG peaks in VCaP cells overlapped with AR peaks (Figure 7A). GO enrichment analysis revealed that regions near common AR and ERG peaks are enriched in genes involved in nucleosome and chromatin assembly (data not shown).

We further performed comparisons with earlier reports. In all, 171 (51.3%) of total 333 ELF1-specific occupancy regions discovered by ChIP-chip in Jurkat (Hollenhorst *et al*, 2007) overlapped with our ELF1 ChIP-seq peaks. For comparison, we also analysed overlap of our ELF1 ChIP-seq peaks with recent ChIP-seq data of the ETS-family members ETS1 and GABPA in Jurkat cells (Valouev *et al*, 2008; Hollenhorst *et al*, 2009) (see Materials and methods; Supplementary Table S4 for details). Earlier studies showed the redundant occupancy of the ETS-family members at promoter proximal regions (Hollenhorst *et al*, 2007, 2009). Indeed, comparisons between overlap results from top significant peaks of ETS1, GABPA and ELF1 showed higher overlap of peaks in promoter

regions (Supplementary Table S4). Outside promoters, it appears that there is a higher overlap between class I factor ETS1 and GABPA peaks compared to overlap of either ETS1 or GABPA with the class II factor ELF1 peaks (Supplementary Table S4).

As many ETS-family members are known to form composite sites with other TFs, we also analysed the ERG peaks that overlapped with AR peaks to see whether the strong overlap between ERG and AR could be explained by the presence of such a composite site in the overlapping peaks. MEME analysis of the overlapping peaks yielded separate ETS and AR signatures, with no obvious composite site (Supplementary Figure S8B).

## Discussion

### ETS-binding specificity

We report here the binding specificities of all human and mouse ETS-family TFs. Earlier phylogenetic analyses based on the ETS domains using the CLUSTALW algorithm have classified these factors into 12 different groups (Laudet *et al*, 1999; Hollenhorst *et al*, 2007). We report here that the ETS-domain DNA-binding specificities fall into only four major distinct classes, which we name classes I to IV based on the number of members in each class. Class II is further subdivided into classes IIa and IIb, based on a more subtle change in binding specificity within this group. The binding



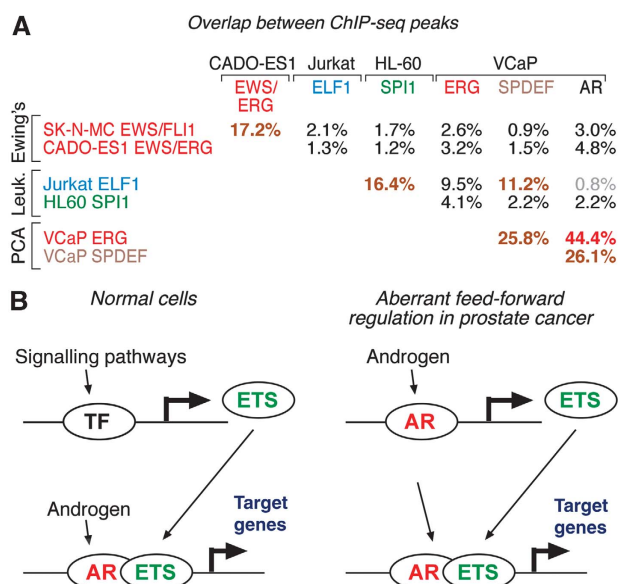


**Figure 7** Analysis of ChIP-seq data. (A) Overlap between ChIP-seq peaks. All overlaps are significantly enriched compared with random expectation ( $P < 0.001$ ), with exception of ELF1 versus AR (in grey, significance  $P = 0.0013$ ).  $P$ -values for each overlap are listed in Supplementary Table S4. Note that the highest observed overlap (red bold typeface) is between AR and ERG. Other overlaps over 10% are coloured in brown. (B) Model of aberrant feed-forward regulation of common androgen receptor and ETS targets in prostate cancer. In normal cells (left), activation of AR and ETS-family TFs requires separate signals. In prostate cancer (right), a strong AR-regulated element is fused to ERG, ETV1 or ETV4 (indicated by ETS), resulting in an aberrant feed-forward loop (arrows) (see also Supplementary Table S4; Supplementary data files S2–S8).

specificity classification we report here is broadly similar to that generated by aligning the ETS-domain peptide sequences from multiple species using the MUST program (Laudet *et al*, 1999) but differs from that generated by ClustalW using just human sequences by Hollenhorst *et al* (2007) or by us (Supplementary Figures S4 and S5). A tree that is more consistent with our binding specificity data was also obtained using the Prank algorithm (Supplementary Figure S6), which uses phylogeny-aware gap placement and scores insertions and deletions more accurately than other alignment programs (Löytynoja and Goldman, 2005, 2008). Alignment analysis of the ETS domains by Prank fails only to clearly identify the class II factors as a single group; instead, the class II members are placed in several branches. One possible explanation is that the class II represents the ancestral specificity from where the other classes diverged.

Of the four classes of the ETS factors, crystal structures exist for classes I, IIa, III and IV. Our results are consistent with these structures, and the changes in binding specificity correlate with changes in amino acids contacting DNA at or near the base pairs affected (Figure 5). Our results also suggest that further structural studies of ETS factors should concentrate on class IIb factors, and cocrystals between ETS factors and other TFs.

Earlier studies have suggested that further specificity exists within the class I ETS DBDs; Elk4 has been reported to have higher specificity towards sequence ACAGGATGT than Elk1 (reviewed in Verger and Duterque-Coquillaud, 2002). These earlier results are based on SELEX with only 11 and 20

sequences analysed (Shore and Sharrocks, 1995; Shore *et al*, 1996) and are not statistically significant (not shown). We do not observe significant differences between Elk1 and Elk4 DNA-binding specificity in either of the independently performed DNA-binding specificity assays, suggesting that the differences in binding observed earlier were related to changes in overall affinity of the ETS factors to DNA as opposed to effect on specificity of binding to different sequences. This interpretation is also supported by existing crystal structure data (Mo *et al*, 1998), which indicates that Tyr 65 of Elk4 makes base-specific contacts with both T and A at +4, whereas the corresponding tyrosine in Elk1 does not contact DNA at all. This should result in lower overall affinity of Elk1 to DNA.

The broad biological functions of the distinct classes of ETS factors do not appear to be clearly separate, for example class I, IIb and III factors are all involved in hematopoiesis, albeit at different steps (Bartel *et al*, 2000). Further class-specific functions could, however, be revealed by combining multiple knockouts within the same ETS class. Gain-of-function evidence does suggest that there is some class specificity in biological functions, as only class I ETS DBDs are found in cancer-associated fusion proteins. Further analysis of the critical targets of the oncogenic ETS factors is needed to reveal the basis of this selectivity.

### Assay bias revealed by systematic analysis of binding specificities

Existing information seems to indicate that different ETS-family members have divergent binding specificities, and no clear subgroups could be identified based on clustering of the existing binding profiles (Figure 3C). Our results show that the previously observed differences are largely attributable to experimental variation and different methods used rather than actual differences in specificity. Similarly, individually analysed homeobox-TF-binding profiles were found to be more divergent compared with those reported in two systematic studies (Berger *et al*, 2008; Noyes *et al*, 2008). Given the diversity of the currently available binding profiles, even for the same factors (see Figure 3C), it is important that systematic approaches such as those described here are extended to all TFs.

These results also highlight the improved precision and accuracy that can be obtained in high-throughput experiments, where all experiments are similarly designed and carefully controlled. Protein–DNA interaction analyses necessarily measure a relatively large number of individual affinities. This makes the assay type and laboratory variation inherent in single-protein studies more apparent than comparison between high-throughput and single-protein studies in other fields (such as protein–protein interactions, where only one  $K_d$  is measured).

The differences between our completely independently performed microwell and PBM assays were relatively small, and comparison using either data set alone did not reveal more classes of factors than comparisons including all data (see Supplementary Figure S1A). However, principal component analysis of the matrices could be used to separate matrices based on the assay used (see Supplementary Figure S1B). Thus, there was a minor systematic difference between microwell and PBM-derived matrices, but its

magnitude was so small that it is unlikely to affect downstream analyses.

### ChIP-seq analyses

The ChIP-seq experiments confirmed that the *in vitro* specificity analyses were relevant also for TF-binding *in vivo* (Figure 6C and D). We found that high-affinity sites were strongly enriched near the summits of the ChIP-seq peaks, and that a substantial fraction of high-affinity sites within accessible genomic regions were occupied (Supplementary Table S4). In addition, comparison of ChIP-seq data to expression profiling data revealed that only a small fraction of FLI1 ChIP-seq peaks are located in close proximity to genes that are strongly regulated by loss of FLI1. Whereas FLI1 peaks were located randomly with respect to transcription start sites, enrichment of FLI1 peaks near FLI1-target genes was clearly higher near the TSS (Figure 6B). It thus appears that most occupied sites have little if any effect on gene expression, and that proximity of the occupied site to a TSS is important in determining whether an ETS binding event affects transcription. However, it is well established that long-range enhancers have pivotal functions in mammalian gene regulation (Heintzman and Ren, 2009), and our results do not mean that all distal sites are non-functional.

Although overlap was observed between the different ETS classes, most of the peaks observed were specific for a given factor, underscoring the specificity of the ETS-family members. A notable exception was found in the VCaP prostate cancer cell line. Activity of two classes of TFs, the AR, and the class I ETS factors ERG, ETV1 and/or ETV4 are implicated in prostate cancer. We found here that a very large fraction (44.4%) of ERG occupied sites are close to sites occupied by AR, and 30.4% of these sites are also bound by SPDEF (not shown). These results suggest that the translocation/deletion that places a strong androgen-responsive element from the TMPRSS2 gene adjacent to the ERG-coding sequences will result in aberrant feed-forward regulation of target genes common to both AR and ERG (Figure 7B).

### Basis of specificity of TFs

The human genome contains large number of TFs contributing to complex gene regulation, accurate developmental patterning and growth control (Messina *et al*, 2004). Many classes of TFs, including members of the ETS and HOX families have relatively similar binding specificities (Berger *et al*, 2008; Noyes *et al*, 2008). Despite similar specificities and overlapping expression patterns (Galang *et al*, 2004; Hollenhorst *et al*, 2004; Richardson *et al*, 2010; Supplementary Figure S7), loss-of-function studies have revealed that ETS-family TFs have very specific functions during development (Bartel *et al*, 2000). An important question is how such specificity is achieved despite relatively similar DNA-binding specificity.

We provide here direct evidence that even the relatively small differences in ETS-domain DNA-binding specificity affect *in vivo* site occupancy. Although the consensus sequences of the ETS factors are very similar, many somewhat weaker sites are much more class specific or exclude one or more classes of ETS DBDs (Supplementary Figure S2). Such selectivity is clearly evident also in our ChIP-seq analyses; we found clear enrichment of class I ETS-binding sites over binding sites of the other classes in regions immunoprecipi-

tated by the class I ETS-family members ERG and FLI1. Similar enrichments were observed for all the other classes as well (Figure 6C). These results indicate that the ETS-class specificities reported here contribute to site selectivity of the ETS-family TFs *in vivo*.

Whereas it is possible that more sensitive methods could, in the future, be used to further subdivide ETS-domain DNA-binding specificities, such differences would necessarily be even smaller than those reported here. Thus, it appears that DNA-binding specificity differences alone cannot explain the full diversity of the ETS family, as there are 27 ETS TFs and four major classes of DNA-binding specificity. One common mechanism explaining how loss of similar proteins can cause different phenotypes is that their expression patterns are different. In mouse embryos, the ETS-family members show distinct but partially overlapping expression patterns (Supplementary Figure S7), suggesting that at least part of the functional specialization within the classes can be explained by the divergent expression patterns (Richardson *et al*, 2010). This hypothesis is also supported by knock-in experiments that show that the class III ETS factor SPIB can replace another class III factor SPI1 (SFPI1) in mouse myeloid development (Dahl *et al*, 2002; DeKoter *et al*, 2002). In contrast, the class I ETS factor ETS1 cannot rescue SFPI1 loss.

Another important mechanism to achieve specificity involves cooperative binding of ETS factors with other TFs. The protein-binding surfaces of ETS factors are different, and different ETS factors associate with different other TFs to bind distinct composite sites (Verger and Dutertre-Coquillaud, 2002). For example, the class I factors ETS1, ELK1, ELK4 and FLI1 have different binding partners. ELK1 or ELK4 can bind DNA together with SRF (Dalton and Treisman, 1992; Cooper *et al*, 2007; Boros *et al*, 2009), FLI1 associates with SMAD3 (Ravasi *et al*, 2010) and ETS1 can bind to composite sites with PAX5 (Garvie *et al*, 2001) and RUNX1 (Hollenhorst *et al*, 2007, 2009). In the cases analysed, the composite sites are distinct from ETS consensus sequences either at the flanking regions, or even at the core region. ETS1 and PAX5 interact to recognize an element containing a modified ETS core sequence GGAG instead of the consensus GGA(A/T) (Fitzsimmons *et al*, 1996, 2001; Garvie *et al*, 2001).

Formation of the composite sites can affect also *in vivo* binding specificity, and this has been demonstrated in the case of ETS1/RUNX1 (Hollenhorst *et al*, 2009). Although such cooperative interactions could potentially explain the differences we observe in *in vivo* binding for the members of the different ETS classes, we did not find obvious motifs corresponding to other TFs in our MEME analysis of the ETS factors ERG, EWS/ERG, EWS/FLI1, ELF1, SPI1 and SPDEF. This suggests that these factors partner with multiple TFs in such a way that any given composite site is present in relatively small numbers—and thus cannot be detected by the algorithm used. Improvement of methods to systematically map such interactions between ETS-family members and other TFs is needed to fully understand *in vivo* specificity differences within each ETS class.

Taken together, in this work, we systematically analysed the ETS family of TF DNA-binding specificities for two species (human and mouse) with a single high-throughput assay (microwell based). The DNA-binding specificities of ETS-family TFs in the mouse genome were determined by two

independent methods (microwell based and PBM). Both sets of *in vitro* data are consistent and reveal four clear subclasses of ETS DNA-binding preferences. We further dissected molecular basis for the specificity in DNA recognition by systematic site-directed mutagenesis of key amino acids in the ETS DBDs. Through ChIP-seq mapping of ETS-binding sites in different cell models, we found that the preferences observed for ETS DNA-binding *in vitro* can contribute to site selectivity *in vivo* on a genome-wide scale.

## Materials and methods

### Cell culture

SK-N-MC cells were grown in EMEM, Jurkat, HL60, CADO-ES1 in RPMI1640, and COS1, 293T and VCaP in DMEM. All media were supplemented with penicillin/streptomycin and fetal bovine serum (10%).

### Cloning

Sequences coding for the human and mouse ETS domains with 10–25 amino acids of flanking sequence (with exception of ETS domains in N- or C-terminal regions) were cloned into pMAGIC1 (Li and Elledge, 2005) or directly to pGEN expression vector (Taipale *et al*, 2002) from Megaman cDNA library (Stratagene) and from mouse-pooled cDNAs (mouse 12.5 days embryonic and fetal brain cDNA library; a kind gift from Professor Tomi Mäkelä, University of Helsinki). The inserts in pMAGIC1 were transferred to pMAGIC-DEST vector containing C-terminal *Renilla* luciferase. All the human ETS full-length cDNAs were cloned into Gateway pDONR221 vector. For expression analyses, the clones were transferred into modified pDEST40 (Invitrogen) vectors containing C-terminal triple V5 or *Renilla* luciferase tags.

### Validation of high-throughput data

Validation of high-throughput data was performed as follows: TF-binding assays were performed using two different methods in two different laboratories. The ChIP analyses were validated using single ChIP-qPCR with different antibodies for 11–42 randomly selected peaks (Supplementary Table S5). In expression analysis, two different siRNAs for each factor were used to rule out off-target effects (Echeverri *et al*, 2006), and two biological replicates were used to decrease noise. Thirty-five randomly selected up- or downregulated genes were validated using qPCR (Supplementary Table S5).

### Analysis of TF-binding specificity

Microwell-based TF DNA-binding assay was performed as described (Hallikas and Taipale, 2006). The method is based on competition between binding sites, and measures relative sequence-specific DNA-binding affinity of a TF. Briefly, TF-*Renilla* luciferase fusion proteins expressed in COS1 or 293T cells were incubated with competitor oligonucleotides indicated in the presence of a biotinylated oligonucleotide containing the ETS consensus-binding sequence (Forward: ACGTAACCGGATATAACGCTA; Reverse: TAGCGTTATATCCGGTTAGCGT) (Nye *et al*, 1992; Woods *et al*, 1992; Hallikas *et al*, 2006). A scrambled oligonucleotide (Forward: ACGCTAAACAGTGTCAACGCTA; Reverse: TAGCGTTGACACTGTTTAGCGT) was used to control for non-sequence-specific DNA-binding affinity. Bound TF-*Renilla* luciferase activity was measured using a luminometer (BMG Fluostar Optima) and normalized to yield TF-binding positional weight matrix as described in Hallikas and Taipale (2006). DBDs were used to determine binding profiles, as initial experiments indicated that significant differences were not observed between profiles obtained using full-length proteins or DBDs for GABP $\alpha$  or ETS1 (Supplementary Figure S9A). Biotinylated oligonucleotides with GGAT core sequence were used as this allowed efficient assay in all classes of ETS factors. Control experiments indicated that use of GGAT core instead of GGAA did not markedly affect results (Supplementary Figure S9B). Microwell-based assay was performed using 3–6 replicate measurements for each competing DNA sequence (see Supplementary Table S6) for all factors. Replicate measurements were compared with each other using the novel algorithm described below. Results shown represent

averages from all replicates that were within minimum Kullback–Leibler divergence of 0.5 (see below).

Independent analysis of the mouse ETS family was carried out using PBMs, which analyse binding of TFs to double-stranded DNA microarrays synthesized with all possible 10bp DNA sequences (Berger *et al*, 2006). The ETS TF proteins were purified from *Escherichia coli* or from *in vitro* translation reactions. Binding reactions were performed with 39–100 nM (see Supplementary Table S1) of protein using PBM array design #015681 essentially as described in Berger *et al* (2006).

### Divergence of motifs

Comparison of binding profiles was performed using a novel algorithm that determines the similarity between TF motifs using the minimum Kullback–Leibler divergence between all translations and reverse complementations of the multinomial distributions defined by the motifs. Conceptually, the TF-motif divergence measures the information gained about the DNA sequence by knowledge of having binding sites for both of the two factors. The TF-motif divergence is defined as the minimum Kullback–Leibler divergence between all translations and reverse complementations of the multinomial distributions defined by the two TF motifs. The longer motif is inserted to a sequence with background distribution and the shorter motif is slid over the background/longer motif sequence. The KL divergence is computed between the multinomial distributions defined by (1) the shorter motif and (2) the part of the background/longer motif sequence overlapping the shorter motif. The same is repeated with the background/long motif sequence reverse complemented and the minimum of the KL divergences is taken. The TF-motif divergence is symmetric but does not fulfill the triangle inequality and thus is not a metric in the mathematical sense. The TF motifs are clustered with hierarchical average linkage clustering (Mahony and Benos, 2007) based on the TF-motif divergences. The TF-motif divergence bears similarity to earlier comparison strategies (Roepcke *et al*, 2005; Mahony and Benos, 2007) in the use of KL divergence but as far as we know, taking the minimum is a novel feature.

Four matrices representative of the different ETS classes were selected using affinity propagation clustering (Frey and Dueck, 2007). This method does not derive an average, but identifies the matrix that is most representative of each group (these were used as the class matrices in Figure 2). The exemplar preferences were uniform on all motifs and the common preference was selected to provide pre-chosen number of clusters.

### Chromatin immunoprecipitation and sequencing

ChIP analysis of VCaP, Jurkat, HL60, SK-N-MC and CADO-ES1 was performed as described earlier (Metivier *et al*, 2003) with minor modifications described in Robertson *et al* (2007). For details and antibodies used, please see Supplementary data.

A detailed description of ChIP-seq DNA library preparation and complexity estimation (Supplementary Table S4), peak calling (Audi and Claverie, 1997; Li *et al*, 2008; Nix *et al*, 2008; Laajala *et al*, 2009; Pepke *et al*, 2009), motif analysis by MEME (Bailey and Elkan, 1994) (Figure 6D; Supplementary Figures S8 and S11), motif enrichment in peaks and peak overlap analysis is included in the Supplementary data. Peak positions (NCBI36 coordinates) are in Supplementary data files S2–S9, and sequencing reads are publicly available at NCBI Sequence Read Archive under accession no. SRA014231.

### siRNA treatment and expression profiling

For siRNA knockdown of EWS/FLI1 in SK-N-MC, the individual set of four siRNAs (Qiagen) against each gene were tested for knockdown efficiency by qRT-PCR, and two most effective single siRNAs were used for further experiments (SI00387716 and SI00387730, Qiagen). The selected FLI1 siRNAs, or non-targeting control siRNA (Ctrl-control\_1, SI03650325, Qiagen) were transfected into cells using HiPerFect Transfection Reagent (Cat. 301704, Qiagen). The final siRNA concentration was 10 nM. After 24 h, a second identical transfection was performed, and cells were harvested 48 h later for RNA isolation.

Before expression profiling, the efficiency of downregulation of the target gene and a set of known target genes were validated using real-time PCR (Supplementary Figure S10 and not shown). Expression profiling was performed using Affymetrix human genome U133plus2.0 arrays. A detailed description of array data

analysis (Smyth, 2004; Wu *et al*, 2004; Falcon and Gentleman, 2007) is provided in the Supplementary data.

### Quantitative real-time PCR

For ChIP experiments, enrichments of immunoprecipitated DNA were analysed by Roche LightCycler and Power SYBR Green Master Mix (Applied Biosystems). Relative enrichment of target DNA fragments was determined by calculating the immunoprecipitation efficiency above fragment-specific background (IgG control) followed by normalization to the occupancy level observed in control regions (see Supplementary Table S6 for primers and control regions used).

For expression analysis of RNAi knockdown efficiency, total RNA was reverse transcribed to cDNA using the High Capacity cDNA RT Kit (ABI), using 500 ng total RNA in a 20- $\mu$ l reaction. The reactions were diluted 10-fold, and gene expression levels were determined from 1 to 3  $\mu$ l of the reactions using qPCR as described above. Each gene was analysed at least in triplicate and normalized against endogenous  $\beta$ -actin control.

## References

- Agarkar VB, Babayeva ND, Wilder PJ, Rizzino A, Tahirov TH (2010) Crystal structure of mouse Elf3 C-terminal DNA-binding domain in complex with type II TGF- $\beta$  receptor promoter DNA. *J Mol Biol* **397**: 278–289
- Audic S, Claverie JM (1997) The significance of digital gene expression profiles. *Genome Res* **7**: 986–995
- Bailey TL, Elkan C (1994) Fitting a mixture model by expectation maximization to discover motifs in biopolymers. *Proc Int Conf Intell Syst Mol Biol* **2**: 28–36
- Bartel FO, Higuchi T, Spyropoulos DD (2000) Mouse models in the study of the Ets family of transcription factors. *Oncogene* **19**: 6443–6454
- Batchelor AH, Piper DE, de la Brousse FC, McKnight SL, Wolberger C (1998) The structure of GABP $\alpha$ /beta: an ETS domain-ankyrin repeat heterodimer bound to DNA. *Science* **279**: 1037–1041
- Beitel GJ, Tuck S, Greenwald I, Horvitz HR (1995) The *Caenorhabditis elegans* gene *lin-1* encodes an ETS-domain protein and defines a branch of the vulval induction pathway. *Genes Dev* **9**: 3149–3162
- Berger MF, Badis G, Gehrke AR, Talukder S, Philippakis AA, Pena-Castillo L, Alleyne TM, Mnaimneh S, Botvinnik OB, Chan ET, Khalid F, Zhang W, Newburger D, Jaeger SA, Morris QD, Bulyk ML, Hughes TR (2008) Variation in homeodomain DNA binding revealed by high-resolution analysis of sequence preferences. *Cell* **133**: 1266–1276
- Berger MF, Philippakis AA, Qureshi AM, He FS, Estep III PW, Bulyk ML (2006) Compact, universal DNA microarrays to comprehensively determine transcription-factor binding site specificities. *Nat Biotechnol* **24**: 1429–1435
- Boros J, Donaldson IJ, O'Donnell A, Odrowaz ZA, Zeef L, Lupien M, Meyer CA, Liu XS, Brown M, Sharrocks AD (2009) Elucidation of the ELK1 target gene network reveals a role in the coordinate regulation of core components of the gene regulation machinery. *Genome Res* **19**: 1963–1973
- Brunner D, Ducker K, Oellers N, Hafen E, Scholz H, Klambt C (1994) The ETS domain protein pointed-P2 is a target of MAP kinase in the sevenless signal transduction pathway. *Nature* **370**: 386–389
- Byrne JC, Valen E, Tang MH, Marstrand T, Winther O, da Piedade I, Krogh A, Lenhard B, Sandelin A (2008) JASPAR, the open access database of transcription factor-binding profiles: new content and tools in the 2008 update. *Nucleic Acids Res* **36**: D102–D106
- Bult CJ, Eppig JT, Kadin JA, Richardson JE, Blake JA, Mouse Genome Database Group (2008) The Mouse Genome Database (MGD): mouse biology and model systems. *Nucleic Acids Res* **36**: D724–D728
- Choi YS, Sinha S (2006) Determination of the consensus DNA-binding sequence and a transcriptional activation domain for ESE-2. *Biochem J* **398**: 497–507
- Cooper SJ, Trinklein ND, Nguyen L, Myers RM (2007) Serum response factor binding sites differ in three human cell types. *Genome Res* **17**: 136–144
- Dahl R, Ramirez-Bergeron DL, Rao S, Simon MC (2002) Spi-B can functionally replace PU.1 in myeloid but not lymphoid development. *EMBO J* **21**: 2220–2230
- Dalton S, Treisman R (1992) Characterization of SAP-1, a protein recruited by serum response factor to the c-fos serum response element. *Cell* **68**: 597–612
- DeKoter RP, Lee HJ, Singh H (2002) PU.1 regulates expression of the interleukin-7 receptor in lymphoid progenitors. *Immunity* **16**: 297–309
- Delattre O, Zucman J, Plougastel B, Desmaziere C, Melot T, Peter M, Kovar H, Joubert I, de Jong P, Rouleau G (1992) Gene fusion with an ETS DNA-binding domain caused by chromosome translocation in human tumours. *Nature* **359**: 162–165
- Echeverri CJ, Beachy PA, Baum B, Boutros M, Buchholz F, Chanda SK, Downward J, Ellenberg J, Fraser AG, Hacohen N, Hahn WC, Jackson AL, Kiger A, Linsley PS, Lum L, Ma Y, Mathey-Prevot B, Root DE, Sabatini DM, Taipale J *et al* (2006) Minimizing the risk of reporting false positives in large-scale RNAi screens. *Nat Methods* **3**: 777–779
- Falcon S, Gentleman R (2007) Using GOSTats to test gene lists for GO term association. *Bioinformatics* **23**: 257–258
- Fitzsimmons D, Hodsdon W, Wheat W, Maira SM, Wasylyk B, Hagman J (1996) Pax-5 (BSAP) recruits Ets proto-oncogene family proteins to form functional ternary complexes on a B-cell-specific promoter. *Genes Dev* **10**: 2198–2211
- Fitzsimmons D, Lutz R, Wheat W, Chamberlin HM, Hagman J (2001) Highly conserved amino acids in Pax and Ets proteins are required for DNA binding and ternary complex assembly. *Nucleic Acids Res* **29**: 4154–4165
- Frey BJ, Dueck D (2007) Clustering by passing messages between data points. *Science* **315**: 972–976
- Galang CK, Muller WJ, Foos G, Oshima RG, Hauser CA (2004) Changes in the expression of many Ets family transcription factors and of potential target genes in normal mammary tissue and tumors. *J Biol Chem* **279**: 11281–11292
- Gangwal K, Sankar S, Hollenhorst PC, Kinsey M, Haroldsen SC, Shah AA, Boucher KM, Watkins WS, Jorde LB, Graves BJ, Lessnick SL (2008) Microsatellites as EWS/FLI response elements in Ewing's sarcoma. *Proc Natl Acad Sci USA* **105**: 10149–10154
- Garvie CW, Hagman J, Wolberger C (2001) Structural studies of Ets-1/Pax5 complex formation on DNA. *Mol Cell* **8**: 1267–1276
- Golub TR, Barker GF, Bohlander SK, Hiebert SW, Ward DC, Bray-Ward P, Morgan E, Raimondi SC, Rowley JD, Gilliland DG (1995) Fusion of the TEL gene on 12p13 to the AML1 gene on 21q22 in acute lymphoblastic leukemia. *Proc Natl Acad Sci USA* **92**: 4917–4921
- Hallikas O, Palin K, Sinjushina N, Rautiainen R, Partanen J, Ukkonen E, Taipale J (2006) Genome-wide prediction of mammalian enhancers based on analysis of transcription-factor binding affinity. *Cell* **124**: 47–59
- Hallikas O, Taipale J (2006) High-throughput assay for determining specificity and affinity of protein-DNA binding interactions. *Nat Protoc* **1**: 215–222

### Supplementary data

Supplementary data are available at *The EMBO Journal* Online (<http://www.embojournal.org>).

## Acknowledgements

We thank Ritva Nurmi and Sini Miettinen for technical assistance, and EMBL gene core, Uppsala SNP platform and Dr Outi Monni for massively parallel sequencing. This work was supported by the EU FP6 STREP project REGULATORY GENOMICS, Sigrid Jusélius Foundation, Finnish Cancer Organizations, Biocentrum Helsinki, Academy of Finland Center of Excellence in Translational Genome-Scale Biology, and the NEURO program of the Academy of Finland. MFB and MLB were supported by grant R01 HG003985 from NIH/NHGRI to MLB.

## Conflict of interest

The authors declare that they have no conflict of interest.



- Heintzman ND, Ren B (2009) Finding distal regulatory elements in the human genome. *Curr Opin Genet Dev* **19**: 541–549
- Heintzman ND, Stuart RK, Hon G, Fu Y, Ching CW, Hawkins RD, Barrera LO, Van Calcar S, Qu C, Ching KA, Wang W, Weng Z, Green RD, Crawford GE, Ren B (2007) Distinct and predictive chromatin signatures of transcriptional promoters and enhancers in the human genome. *Nat Genet* **39**: 311–318
- Hollenhorst PC, Chandler KJ, Poulsen RL, Johnson WE, Speck NA, Graves BJ (2009) DNA specificity determinants associate with distinct transcription factor functions. *PLoS Genet* **5**: e1000778
- Hollenhorst PC, Jones DA, Graves BJ (2004) Expression profiles frame the promoter specificity dilemma of the ETS family of transcription factors. *Nucleic Acids Res* **32**: 5693–5702
- Hollenhorst PC, Shah AA, Hopkins C, Graves BJ (2007) Genome-wide analyses reveal properties of redundant and specific promoter occupancy within the ETS gene family. *Genes Dev* **21**: 1882–1894
- Karim FD, Urness LD, Thummel CS, Klemsz MJ, McKercher SR, Celada A, Van Beveren C, Maki RA, Gunther CV, Nye JA (1990) The ETS-domain: a new DNA-binding motif that recognizes a purine-rich core DNA sequence. *Genes Dev* **4**: 1451–1453
- Kielbasa SM, Gonze D, Herzog H (2005) Measuring similarities between transcription factor binding sites. *BMC Bioinformatics* **6**: 237
- Kodandapani R, Pio F, Ni CZ, Piccialli G, Klemsz MJ, McKercher S, Maki RA, Ely KR (1996) A new pattern for helix-turn-helix recognition revealed by the PU.1 ETS-domain-DNA complex. *Nature* **380**: 456–460
- Kumar-Sinha C, Tomlins SA, Chinnaiyan AM (2008) Recurrent gene fusions in prostate cancer. *Nat Rev Cancer* **8**: 497–511
- Laajala TD, Raghav S, Tuomela S, Lahesmaa R, Aittokallio T, Elo LL (2009) A practical comparison of methods for detecting transcription factor binding sites in ChIP-seq experiments. *BMC Genomics* **10**: 618
- Lamber EP, Vanhille L, Textor LC, Kachalova GS, Sieweke MH, Wilmanns M (2008) Regulation of the transcription factor Ets-1 by DNA-mediated homo-dimerization. *EMBO J* **27**: 2006–2017
- Laudet V, Hanni C, Stehelin D, Dutreque-Coquillaud M (1999) Molecular phylogeny of the ETS gene family. *Oncogene* **18**: 1351–1359
- Leprince D, Gegonne A, Coll J, de Taisne C, Schneeberger A, Lagrou C, Stehelin D (1983) A putative second cell-derived oncogene of the avian leukaemia retrovirus E26. *Nature* **306**: 395–397
- Li H, Ruan J, Durbin R (2008) Mapping short DNA sequencing reads and calling variants using mapping quality scores. *Genome Res* **18**: 1851–1858
- Li MZ, Elledge SJ (2005) MAGIC, an *in vivo* genetic method for the rapid construction of recombinant DNA molecules. *Nat Genet* **37**: 311–319
- Löytynoja A, Goldman N (2005) An algorithm for progressive multiple alignment of sequences with insertions. *Proc Natl Acad Sci USA* **102**: 10557–10562
- Löytynoja A, Goldman N (2008) Phylogeny-aware gap placement prevents errors in sequence alignment and evolutionary analysis. *Science* **320**: 1632–1635
- Mahony S, Benos PV (2007) STAMP: a web tool for exploring DNA-binding motif similarities. *Nucleic Acids Res* **35**: W253–W258
- Matys V, Kel-Margoulis OV, Fricke E, Liebich I, Land S, Barre-Dirrie A, Reuter I, Chekmenev D, Krull M, Hornischer K, Voss N, Stegmaier P, Lewicki-Potapov B, Saxel H, Kel AE, Wingender E (2006) TRANSFAC and its module TRANSCOMP: transcriptional gene regulation in eukaryotes. *Nucleic Acids Res* **34**: D108–D110
- Mavrothalassitis G, Ghysdael J (2000) Proteins of the ETS family with transcriptional repressor activity. *Oncogene* **19**: 6524–6532
- Messina DN, Glasscock J, Gish W, Lovett M (2004) An ORFeome-based analysis of human transcription factor genes and the construction of a microarray to interrogate their expression. *Genome Res* **14**: 2041–2047
- Metivier R, Penot G, Hubner MR, Reid G, Brand H, Kos M, Gannon F (2003) Estrogen receptor- $\alpha$  directs ordered, cyclical, and combinatorial recruitment of cofactors on a natural target promoter. *Cell* **115**: 751–763
- Mo Y, Vaessen B, Johnston K, Marmorstein R (1998) Structures of SAP-1 bound to DNA targets from the E74 and c-fos promoters: insights into DNA sequence discrimination by Ets proteins. *Mol Cell* **2**: 201–212
- Mo Y, Vaessen B, Johnston K, Marmorstein R (2000) Structure of the elk-1-DNA complex reveals how DNA-distal residues affect ETS domain recognition of DNA. *Nat Struct Biol* **7**: 292–297
- Nix DA, Courdy SJ, Boucher KM (2008) Empirical methods for controlling false positives and estimating confidence in ChIP-Seq peaks. *BMC Bioinformatics* **9**: 523
- Noyes MB, Christensen RG, Wakabayashi A, Stormo GD, Brodsky MH, Wolfe SA (2008) Analysis of homeodomain specificities allows the family-wide prediction of preferred recognition sites. *Cell* **133**: 1277–1289
- Nunn MF, Seeburg PH, Moscovici C, Duesberg PH (1983) Tripartite structure of the avian erythroblastosis virus E26 transforming gene. *Nature* **306**: 391–395
- Nye JA, Petersen JM, Gunther CV, Jonsen MD, Graves BJ (1992) Interaction of murine ets-1 with GGA-binding sites establishes the ETS domain as a new DNA-binding motif. *Genes Dev* **6**: 975–990
- Oettgen P, Finger E, Sun Z, Akbarali Y, Thamrongsak U, Boltax J, Grall F, Dube A, Weiss A, Brown L, Quinn G, Kas K, Endress G, Kunsch C, Libermann TA (2000) PDEF, a novel prostate epithelium-specific ets transcription factor, interacts with the androgen receptor and activates prostate-specific antigen gene expression. *J Biol Chem* **275**: 1216–1225
- O'Neill EM, Rebay I, Tjian R, Rubin GM (1994) The activities of two Ets-related transcription factors required for Drosophila eye development are modulated by the Ras/MAPK pathway. *Cell* **78**: 137–147
- Pepke S, Wold B, Mortazavi A (2009) Computation for ChIP-seq and RNA-seq studies. *Nat Methods* **6**: S22–S32
- Pufall MA, Lee GM, Nelson ML, Kang HS, Velyvis A, Kay LE, McIntosh LP, Graves BJ (2005) Variable control of Ets-1 DNA binding by multiple phosphates in an unstructured region. *Science* **309**: 142–145
- Ravasi T, Suzuki H, Cannistraci CV, Katayama S, Bajic VB, Tan K, Akalin A, Schmeier S, Kanamori-Katayama M, Bertin N, Carninci P, Daub CO, Forrest AR, Gough J, Grimmond S, Han JH, Hashimoto T, Hide W, Hofmann O, Kawaji H et al (2010) An atlas of combinatorial transcriptional regulation in mouse and man. *Cell* **140**: 744–752
- Ray-Gallet D, Mao C, Tavittian A, Moreau-Gachelin F (1995) DNA binding specificities of Spi-1/PU.1 and Spi-B transcription factors and identification of a Spi-1/Spi-B binding site in the c-fes/c-fps promoter. *Oncogene* **11**: 303–313
- Richardson L, Venkataraman S, Stevenson P, Yang Y, Burton N, Rao J, Fisher M, Baldock RA, Davidson DR, Christiansen JH (2010) EMAGE mouse embryo spatial gene expression database: 2010 update. *Nucleic Acids Res* **38**: D703–D709
- Robertson G, Hirst M, Bainbridge M, Bilenky M, Zhao Y, Zeng T, Euskirchen G, Bernier B, Varhol R, Delaney A, Thiessen N, Griffith OL, He A, Marra M, Snyder M, Jones S (2007) Genome-wide profiles of STAT1 DNA association using chromatin immunoprecipitation and massively parallel sequencing. *Nat Methods* **4**: 651–657
- Roepcke S, Grossmann S, Rahmann S, Vingron M (2005) T-Reg Comparator: an analysis tool for the comparison of position weight matrices. *Nucleic Acids Res* **33**: W438–W441
- Schober M, Rebay I, Perrimon N (2005) Function of the ETS transcription factor Yan in border cell migration. *Development* **132**: 3493–3504
- Sharrocks AD (2001) The ETS-domain transcription factor family. *Nat Rev Mol Cell Biol* **2**: 827–837
- Shore P, Sharrocks AD (1995) The ETS-domain transcription factors Elk-1 and SAP-1 exhibit differential DNA binding specificities. *Nucleic Acids Res* **23**: 4698–4706
- Shore P, Whitmarsh AJ, Bhaskaran R, Davis RJ, Waltho JP, Sharrocks AD (1996) Determinants of DNA-binding specificity of ETS-domain transcription factors. *Mol Cell Biol* **16**: 3338–3349
- Smyth GK (2004) Linear models and empirical bayes methods for assessing differential expression in microarray experiments. *Stat Appl Genet Mol Biol* **3**: Article3
- Sorensen PH, Lessnick SL, Lopez-Terrada D, Liu XF, Triche TJ, Denny CT (1994) A second Ewing's sarcoma translocation, t(21;22), fuses the EWS gene to another ETS-family transcription factor, ERG. *Nat Genet* **6**: 146–151
- Taipale J, Cooper MK, Maiti T, Beachy PA (2002) Patched acts catalytically to suppress the activity of Smoothened. *Nature* **418**: 892–897
- Tirode F, Laud-Duval K, Prieur A, Delorme B, Charbord P, Delattre O (2007) Mesenchymal stem cell features of Ewing tumors. *Cancer Cell* **11**: 421–429

- Tomlins SA, Laxman B, Dhanasekaran SM, Helgeson BE, Cao X, Morris DS, Menon A, Jing X, Cao Q, Han B, Yu J, Wang L, Montie JE, Rubin MA, Pienta KJ, Roulston D, Shah RB, Varambally S, Mehra R, Chinnaiyan AM (2007) Distinct classes of chromosomal rearrangements create oncogenic ETS gene fusions in prostate cancer. *Nature* **448**: 595–599
- Tomlins SA, Rhodes DR, Perner S, Dhanasekaran SM, Mehra R, Sun XW, Varambally S, Cao X, Tchinda J, Kuefer R, Lee C, Montie JE, Shah RB, Pienta KJ, Rubin MA, Chinnaiyan AM (2005) Recurrent fusion of TMPRSS2 and ETS transcription factor genes in prostate cancer. *Science* **310**: 644–648
- Treisman R, Marais R, Wynne J (1992) Spatial flexibility in ternary complexes between SRF and its accessory proteins. *EMBO J* **11**: 4631–4640
- Valouev A, Johnson DS, Sundquist A, Medina C, Anton E, Batzoglou S, Myers RM, Sidow A (2008) Genome-wide analysis of transcription factor binding sites based on ChIP-Seq data. *Nat Methods* **5**: 829–834
- Verger A, Duterrque-Coquillaud M (2002) When Ets transcription factors meet their partners. *Bioessays* **24**: 362–370
- Virbasius JV, Virbasius CA, Scarpulla RC (1993) Identity of GABP with NRF-2, a multisubunit activator of cytochrome oxidase expression, reveals a cellular role for an ETS domain activator of viral promoters. *Genes Dev* **7**: 380–392
- Vrieseling E, Arber S (2006) Target-induced transcriptional control of dendritic patterning and connectivity in motor neurons by the ETS gene *Pea3*. *Cell* **127**: 1439–1452
- Wang Y, Feng L, Said M, Balderman S, Fayazi Z, Liu Y, Ghosh D, Gulick AM (2005) Analysis of the 2.0 Å crystal structure of the protein-DNA complex of the human PDEF Ets domain bound to the prostate specific antigen regulatory site. *Biochemistry* **44**: 7095–7106
- Wasylyk C, Bradford AP, Gutierrez-Hartmann A, Wasylyk B (1997) Conserved mechanisms of Ras regulation of evolutionary related transcription factors, Ets1 and Pointed P2. *Oncogene* **14**: 899–913
- Woods DB, Ghysdael J, Owen MJ (1992) Identification of nucleotide preferences in DNA sequences recognised specifically by c-Ets-1 protein. *Nucleic Acids Res* **20**: 699–704
- Workman CT, Yin Y, Corcoran DL, Ideker T, Stormo GD, Benos PV (2005) enoLOGOS: a versatile web tool for energy normalized sequence logos. *Nucleic Acids Res* **33**: W389–W392
- Wu Z, Irizarry RA, Gentleman R, Martinez-Murillo F, Spencer F (2004) A model-based background adjustment for oligonucleotide expression arrays. *J Am Stat Assoc* **99**: 909–917



The EMBO Journal is published by Nature Publishing Group on behalf of European Molecular Biology Organization. This article is licensed under a Creative Commons Attribution-NonCommercial-Share Alike 3.0 Unported License. [<http://creativecommons.org/licenses/by-nc-sa/3.0/>]